

## Supporting Information

### **A cascade Fermat spiral microfluidic mixer chip for accurate detection and logic discrimination of cancer cells**

Shiyu Zeng,<sup>‡<sup>a</sup></sup> Xiaocheng Sun,<sup>‡<sup>b</sup></sup> Xinhua Wan,<sup>‡<sup>a</sup></sup> Changcheng Qian,<sup>a</sup> Wenkai Yue,<sup>a</sup> A S M Muhtasim Fuad Sohan,<sup>a</sup> Xiaodong Lin,<sup>b\*</sup> Binfeng Yin<sup>a\*</sup>

<sup>a</sup> School of Mechanical Engineering, Yangzhou University, Yangzhou 225127, China

<sup>b</sup> College of Food and Biological Engineering, Zhengzhou University of Light Industry, Zhengzhou 450001, China

E-mail: binfengyin@yzu.edu.cn (Binfeng Yin), lxdxf2011@163.com (Xiaodong Lin)

Tel.: (+86) 514-87978347

Fax: (+86) 514-87311374

### ***Contents***

Additional file 1: Fig. S1

Additional file 2: Fig. S2

Additional file 3: Fig. S3

Additional file 4: Fig. S4

Additional file 5: Fig. S5

Additional file 6: Table S1

Additional file 7: Table S2



**Fig. S1.** The molds of dual PDMS layers are manufactured by SLA 3D printer.



**Fig. S2.** The construction of Casade Fermat Spiral Microfluidic Chip. Assembly drawing of the fabricated push valve, cured dual PDMS layer.

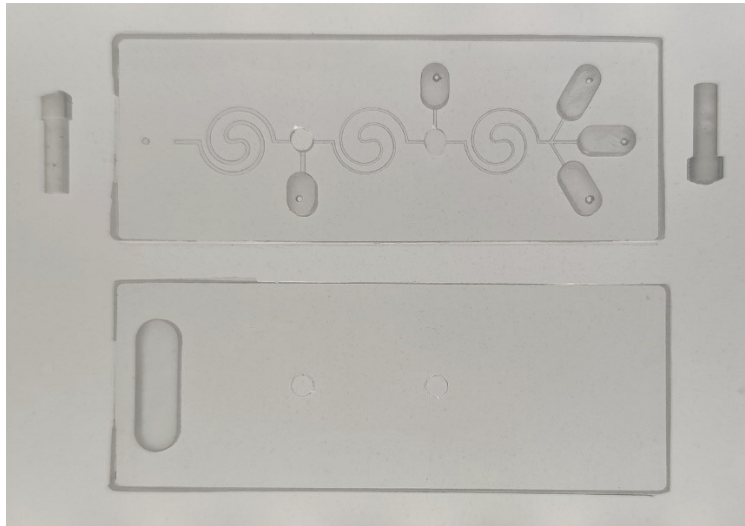


**Fig. S3.** The cured dual PDMS layers (the Microchannel layer and base layer).

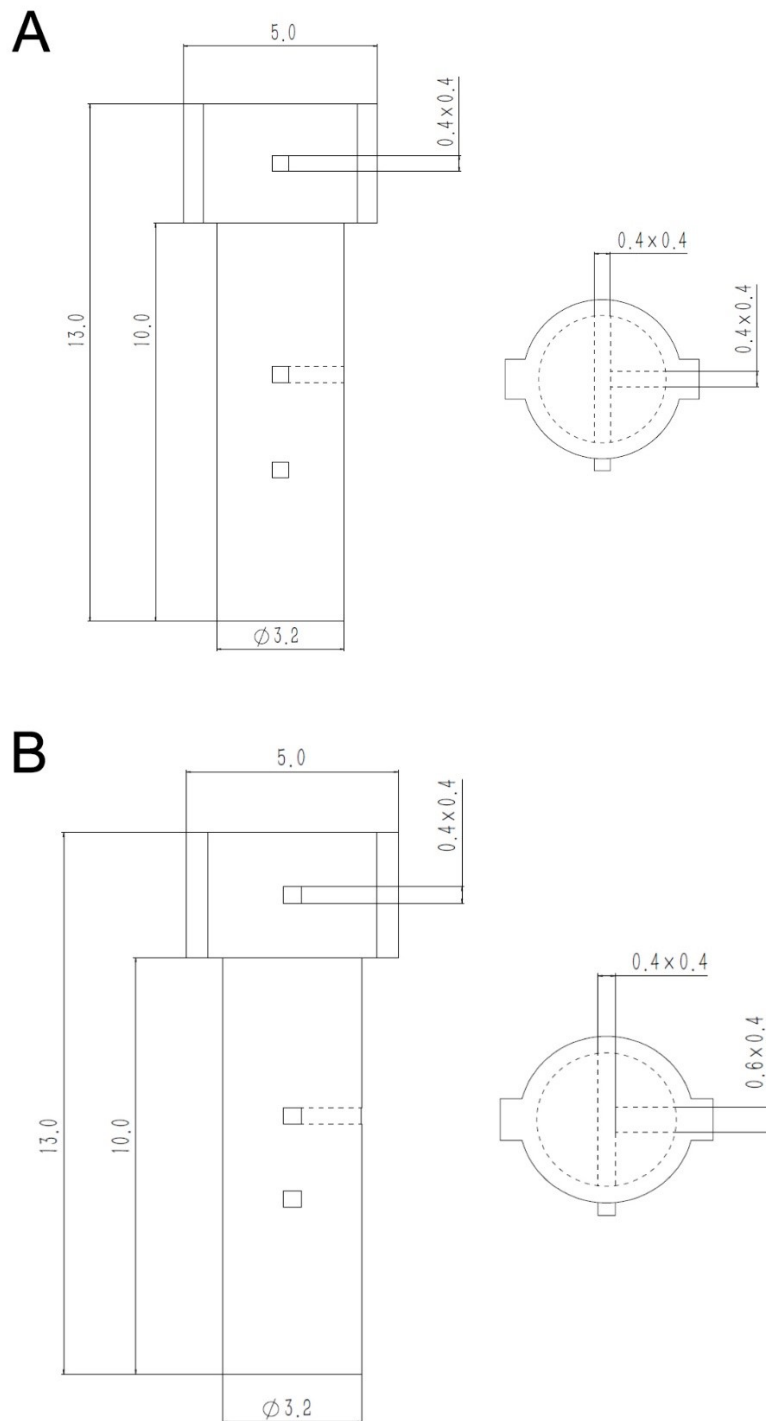


**Fig. S4.** The two-dimensional (2D) drawing of push valve on the left (A) and right (B) sides of the microfluidic chip. It showed the push valve on the left side of the microfluidic chip (A). The push valve had a total length of 13 mm and was divided into two parts: the valve head and the valve body. The valve head is 3 mm long and 5 mm wide, and there was a  $0.4 \times 0.4$  mm protrusion on the valve

head for positioning when installing push valves. The valve body was 10 mm long and 3.2 mm in diameter, and there were two sets of through holes on the valve body for realizing the flow of liquid. The upper hole was a T-shaped through hole of  $0.4 \times 0.4$  mm, and the lower hole was a straight through hole of  $0.4 \times 0.4$  mm. To ensure that the cancer cells do not block when entering the microchannel, the microchannel connected to the cancer cell reservoir in the upper side hole was designed as a  $0.6 \times 0.4$  mm through-hole to ensure smooth sample feeding (B), and the rest of the hole design was consistent with Fig.S4 A.

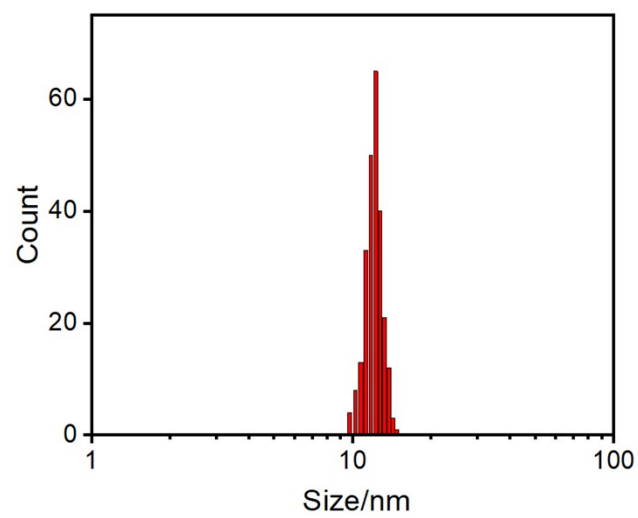


**Fig. S5.** The particle size statistical analysis of AuNPs

**Table S1. The local section and maximum errors of CFSMM.**

<b>Local section of CFSMM</b>	<b>Design size (<math>\mu\text{m}</math>)</b>	<b>Actual size (<math>\mu\text{m}</math>)</b>	<b>Maximum error (<math>\mu\text{m}</math>)</b>	<b>Maximum error Percentage (%)</b>
a	400 wide	397.85 408.35	9.73	2.43
		390.27 404.63		
b	400 wide	395.74	4.26	1.07
	400 deep	397.68		
c	400 wide	391.17	8.83	2.21
d	400 wide	388.61	11.39	2.85
e	600 wide	607.72	7.72	1.29
f	600 wide	611.92	11.92	1.99
	400 deep	390.81		

The data in Table S1 are originally from Figure 1B.



**Table S2. Comparison of CFSMMC detection capabilities.**

Method	Cell types	Limit of Detection	References
Colorimetric	SKBR-3 cells	100 cells/mL	[1]
Colorimetric	MCF-7 cells	125 cells/mL	[2]
Colorimetric	CCRF-CEM cells	40 cells/mL	[3]
Electrochemical	A-549 lung cancer cells	25 cell/mL	[4]
Electrochemical	HeLa cells	273 cell/mL	[5]
microcantilever	HepG2 cells	300 cell/mL	[6]
Electrochemical	MCF-7 cells	19 cells/mL	[7]
Fluorescence	CCRF-CEM cells	44 cells/mL	[8]
Fluorescence	MCF-7 cells	17 cells/mL	This work

## References

- [1] Moon Il Kim, Min Su Kim, Min Ah Woo, Youngjin Ye, Kyoung Suk Kang, Jinwoo Lee, and Hyun Gyu Park. Highly efficient colorimetric detection of target cancer cells utilizing superior catalytic activity of graphene oxide-magnetic-platinum nanohybrids, *Nanoscale*, 2014,**6**, 1529-1536.
- [2] Lingna Zhang, Haohua Deng, Fenglin Lin, Xiongwei Xu, Shaohuang Weng, Ailin Liu, Xinhua Lin, Xinghua Xia, and Wei Chen, In situ growth of porous platinum nanoparticles on graphene oxide for colorimetric detection of cancer cells, *Analytical Chemistry*, 2014, **86**, 5, 2711-2718.

- [3] Xianxia Zhang, Kunyi Xiao, Liwei Cheng, Hui Chen, Baohong Liu, Song Zhang, and Jilie Kong. Visual and highly sensitive detection of cancer cells by a colorimetric aptasensor based on cell-triggered cyclic enzymatic signal amplification, *Analytical Chemistry*, 2014, **86**, 11, 5567-5572.
- [4] Gulcin Bolat, Oznur Akbal Vural, Yesim Tugce Yaman, Serdar Abaci. Polydopamine nanoparticles-assisted impedimetric sensor towards label-free lung cancer cell detection, *Materials Science and Engineering: C*, 2021, **119**, 111549.
- [5] Ankan Dutta Chowdhury, Akhilesh Babu Ganganboinab, Yuanchung Tsai, Hsincheng Chiu, and Rueyan Doong. Multifunctional GQDs-Concanavalin A@Fe<sub>3</sub>O<sub>4</sub> nanocomposites for cancer cells detection and targeted drug delivery, *Analytica chimica acta*, 2018, **1027**, 109-120.
- [6] Xuejuan Chen, Yangang Pan, Huiqing Liu, Xiaojing Bai, Nan Wang, Bailin Zhang. Label-free detection of liver cancer cells by aptamer-based microcantilever biosensor. *Biosensors and Bioelectronics*, 2016, **79**, 353-358.
- [7] Minghua Wang, Mengyao Hu, Zhenzhen Li, Linghao He, Yingpan Song, Qiaojuan Jia, Zhihong Zhang, Miao Du. Construction of Tb-MOF-on-Fe-MOF conjugate as a novel platform for ultrasensitive detection of carbohydrate antigen 125 and living cancer cells. *Biosensors and Bioelectronics*, 2019, **142**, 111536.
- [8] Linchen Ho, Weicheng Wu, Changyu Chang, Hao Hsuan Hsieh, Ching Hsiao Lee, Huan Tsung Chang. Aptamer-conjugated polymeric nanoparticles for the detection of cancer cells through “turn-on” retro-self-quenched fluorescence. *Analytical chemistry*, 2015, **87**, 4925-4932.